REPORT DOCUMENTATION PAGE

Form Approved OMB NO. 0704-0188

1. REPORT DATE (DD-MM-YYYY)	2. REPORT TYPE	3. DATES COVERED (From - To)
13-07-2010	Final Report	1-May-2005 - 30-Sep-2009

4. TITLE AND SUBTITLE

RESPONSES & MODELING OF ELECTRON BEAM SINGLE MELT Ti-6Al-4V ALLOYS

5a. CONTRACT NUMBER
W911NF-05-1-0208

5b. GRANT NUMBER

5c. PROGRAM ELEMENT NUMBER
611102

6. AUTHORS

Akhtar S. Khan

5d. PROJECT NUMBER

5e. TASK NUMBER

5f. WORK UNIT NUMBER

7. PERFORMING ORGANIZATION NAMES AND ADDRESSES

University of Maryland - Baltimore County
Office of Sponsored Programs
Univeristy of Maryland, Baltimore County
Baltimore, MD 21250 -

8. PERFORMING ORGANIZATION REPORT NUMBER

9. SPONSORING/MONITORING AGENCY NAME(S) AND ADDRESS(ES)

U.S. Army Research Office
P.O. Box 12211
Research Triangle Park, NC 27709-2211

10. SPONSOR/MONITOR'S ACRONYM(S)
ARO

11. SPONSOR/MONITOR'S REPORT NUMBER(S)
48443-EG.1

12. DISTRIBUTION AVAILIBILITY STATEMENT

Approved for Public Release; Distribution Unlimited

13. SUPPLEMENTARY NOTES

The views, opinions and/or findings contained in this report are those of the author(s) and should not contrued as an official Department of the Army position, policy or decision, unless so designated by other documentation.

14. ABSTRACT

During a projectile penetrating an armor, the material undergoes finite plastic deformation at high strain rates and temperatures, as well as at high hydrostatic pressures. US Army is contemplating on making a light tank using electron beam single melt titanium alloy as one of the metallic components. The manufacturing process of electron beam single melt results in a more economical version of the titanium alloy than the conventional alloy used in the aerospace application. Thus in this comprehensive study, quasi-static and dynamic uniaxial and multiaxial

15. SUBJECT TERMS

Dynamic loading, High strain rate, Split Hopkinson Bar, Constitutive Modeling, High Temperature, Multiaxial Loading

16. SECURITY CLASSIFICATION OF:			17. LIMITATION OF ABSTRACT	15. NUMBER OF PAGES	19a. NAME OF RESPONSIBLE PERSON
a. REPORT	b. ABSTRACT	c. THIS PAGE			Akhtar Khan
UU	UU	UU	UU		19b. TELEPHONE NUMBER: 410-455-3301

Report Title

RESPONSES & MODELING OF ELECTRON BEAM SINGLE MELT Ti-6Al-4V ALLOYS

ABSTRACT

During a projectile penetrating an armor, the material undergoes finite plastic deformation at high strain rates and temperatures, as well as at high hydrostatic pressures. US Army is contemplating on making a light tank using electron beam single melt titanium alloy as one of the metallic components. The manufacturing process of electron beam single melt results in a more economical version of the titanium alloy than the conventional alloy used in the aerospace application. Thus in this comprehensive study, quasi-static and dynamic uniaxial and multiaxial experimental results on electron beam single melt titanium alloys and one extra low interstitial (ELI) grade (for comparison) are presented, over low to high strain rates and temperatures, as well as under confining hydrostatic pressures. These experiments include compression, tension and torsion, as well as strain-rate jump experiments, in rolling (RD), transverse to rolling (TD) and thicknoess (ND) directions to quantify anisotropy of the plate material. Failure strains at different strain rates and different temperatures, in tension, compression and shear loading are also given. Microstructure is measured using an optical microscope and SEM. Material constants are determined for Johnson-Cook (J-C) & Khan-Huang-Liang (KHL) models, and observations are correlated with these models. Anisotropy in the material is fully characterized. Response of the material under confining pressures is also determined.

List of papers submitted or published that acknowledge ARO support during this reporting period. List the papers, including journal references, in the following categories:

(a) Papers published in peer-reviewed journals (N/A for none)

1. Akhtar S. Khan, Rehan Kazmi & Babak Farrokh, “Multiaxial & non-proportional loading response, anisotropy and modeling of Ti-6Al-4V titanium alloy over wide ranges of strain rates and temperatures”, International Journal of Plasticity, Vol. 23, pp. 931-950, 2007.

2. Akhtar S. Khan, Rehan Kazmi, Babak Farrokh and Marc Zupan, “Effect of oxygen content and microstructure on the thermo-mechanical response of three Ti-6Al-4V alloys: experiments and modeling over a wide range of strain-rates and temperatures”, International Journal of Plasticity, Vol. 23, pp. 1105-1125, 2007.

Number of Papers published in peer-reviewed journals: 2.00

(b) Papers published in non-peer-reviewed journals or in conference proceedings (N/A for none)

Number of Papers published in non peer-reviewed journals: 0.00

(c) Presentations

1. Akhtar S. Khan, Rehan Kazmi, "Response and Modeling of Polymers and Metals Over a Wide Ranges of Strain-rate and Temperatures", Key-note presentation at The Twelfth International Symposium on Plasticity and its Current Applications, Halifax, NS, Canada, July 17-22, 2006.

2. Akhtar S. Khan and Rehan Kazmi, "Measured responses of polymers & titanium alloys over wide ranges of strain rates & temperatures, and a unified modelling of the measured responses", Key-note presentation at The Thirteenth International Symposium on Plasticity and its Current Applications, Girdwood, Alaska, USA, June 2-6, 2007.

3. Akhtar S. Khan, R. Kazmi, B. Farrokh and M. Baig, "Response and constitutive modeling of polymers, and FCC, BCC & HCP metals over wide ranges of grain size, strain rate and temperature",
Key-note presentation at The Fourteenth International Symposium on Plasticity and its Current Applications, Kailua/Kona, Hawaii, USA, January 3-8, 2008.

4. Akhtar S. Khan, R. Kazmi & B. Farrokh, "From conventional metals to emerging materials (polymers & nanocrystalline solids):Responses over wide ranges of strain-rates & temps. and constitutive modeling", Key-note presentation at The Fifteenth International Symposium on Plasticity and its Current Applications, St Thomas, Virgin Islands, USA, January 3-8, 2009.

Number of Presentations: 4.00

Non Peer-Reviewed Conference Proceeding publications (other than abstracts):

Rehan Kazmi and Akhtar S. Khan, "MULTIAXIAL LOADING RESPONSE AND MODELING OF TI-6AL-4V TITANIUM ALLOY", in "Anisotropy, Texture, Dislocations and Multiscale Modeling in Finite Plasticity & Viscoplasticity, and Metal Forming", pp. 142-145, NEAT Press, Fulton, 2006.

Rehan Kazmi, Babak Farrokh and Akhtar S. Khan, "THERMO-MECHANICAL RESPONSE OF TI-6AL-4V ALLOY: EXPERIMENTS AND MODELING OVER A WIDE RANGE OF STRAIN-RATES AND TEMPERATURES", in "Anisotropy, Texture, Dislocations and Multiscale Modeling in Finite Plasticity & Viscoplasticity, and Metal Forming", pp. 148-150, NEAT Press, Fulton, 2006.

Number of Non Peer-Reviewed Conference Proceeding publications (other than abstracts): 2

Peer-Reviewed Conference Proceeding publications (other than abstracts):

Number of Peer-Reviewed Conference Proceeding publications (other than abstracts): 0

(d) Manuscripts

Akhtar S. Khan and Shaojuan Yu, "Anisotropic Responses and Constitutive Modeling of Electron Beam Single Melt Ti-6Al-4V Alloys".

Akhtar S. Khan and Haowen Liu, "A New Anisotropic Failure Criterion for HCP METals".

Number of Manuscripts: 2.00

Patents Submitted

Patents Awarded

Graduate Students

NAME	PERCENT_SUPPORTED
Rehan Kazmi	0.25
Amit Pandey	0.50
Shaojuan Yu	1.00
Haowen Liu	0.25
FTE Equivalent:	**2.00**
Total Number:	**4**

Names of Post Doctorates

NAME	PERCENT_SUPPORTED
Mohammad Abdel-Karim	0.10
Rehan Kazmi	0.10
Babak Farrokh	0.75
FTE Equivalent:	**0.95**
Total Number:	**3**

Names of Faculty Supported

NAME	PERCENT_SUPPORTED	National Academy Member
Akhtar Khan	0.25	No
FTE Equivalent:	**0.25**	
Total Number:	**1**	

Names of Under Graduate students supported

NAME	PERCENT SUPPORTED
FTE Equivalent:	
Total Number:	

Student Metrics

This section only applies to graduating undergraduates supported by this agreement in this reporting period

The number of undergraduates funded by this agreement who graduated during this period:	0.00
The number of undergraduates funded by this agreement who graduated during this period with a degree in science, mathematics, engineering, or technology fields:.....	0.00
The number of undergraduates funded by your agreement who graduated during this period and will continue to pursue a graduate or Ph.D. degree in science, mathematics, engineering, or technology fields:.....	0.00
Number of graduating undergraduates who achieved a 3.5 GPA to 4.0 (4.0 max scale):	0.00
Number of graduating undergraduates funded by a DoD funded Center of Excellence grant for Education, Research and Engineering:	0.00
The number of undergraduates funded by your agreement who graduated during this period and intend to work for the Department of Defense	0.00
The number of undergraduates funded by your agreement who graduated during this period and will receive scholarships or fellowships for further studies in science, mathematics, engineering or technology fields:	0.00

Names of Personnel receiving masters degrees

NAME
Total Number:

Names of personnel receiving PHDs

NAME	
Rehan Kazmi	
Babak Farrokh	
Amit Pandey	
Total Number:	**3**

Names of other research staff

NAME	PERCENT SUPPORTED
FTE Equivalent:	
Total Number:	

Sub Contractors (DD882)

Inventions (DD882)

Final Progress Report
Proposal No.: 48443-EG

TABLE OF CONTENTS

Final Progress Report
Proposal No.: 48443-EG

RESPONSE & MODELING OF ELECTRON BEAM SINGLE MELT Ti-6Al-4V ALLOYS

Principal Investigator: Akhtar S. Khan
Department of Mechanical Engineering
University of Maryland, Baltimore County

ABSTRACT

During a projectile penetrating an armor, the material undergoes finite plastic deformation at high strain rates and temperatures, as well as at high hydrostatic pressures. US Army is contemplating on making a light tank using electron beam single melt titanium alloy as one of the metallic components. The manufacturing process of electron beam single melt results in a more economical version of the titanium alloy than the conventional alloy used in the Aerospace application. Thus in this comprehensive study, quasi-static and dynamic uniaxial and multiaxial experimental results on electron beam single melt titanium alloys and one extra low interstitial (ELI) grade (for comparison) are presented, over low to high strain rates and temperatures, as well as under confining hydrostatic pressures. These experiments include compression, tension and torsion, as well as strain-rate jump experiments, in rolling (RD), transverse to rolling (TD) and thickness (ND) directions to quantify anisotropy of the plate material. Microstructure is measured using an optical microscope and SEM. Material constants are determined for Johnson-Cook (J-C) & Khan-Huang-Liang (KHL) models, and observations are correlated with these models. Anisotropy in the material is fully characterized. Response of the material under confining pressures is also determined.

RESEARCH OBJECTIVES/PROBLEMS STUDIED

The objectives of the research are three-fold; first, to provide responses of these alloys over wide ranges of strain rates and temperatures, especially under multi-axial dynamic loading; second, to provide material constants for the Johnson-Cook and Khan-Huang-Liang models for use in armor penetration modeling, and finally to determine mechanism of deformation in the three alloys.

APPROACH

1. Quasi-static and dynamic **uniaxial** experiments were performed in electron beam single melt titanium alloys and one extra low interstitial (ELI) grade (for comparison), with different oxygen contents, over a strain-rate range of 10^{-6} to 10^{4} s^{-1} and a

temperature range of –100^{o} F to 900^{o} F. These experiments included compression, tension and torsion, as well as strain-rate jump experiments. Microstructure is measured using optical microscope and SEM. Material constants are determined for Johnson-Cook (J-C) & Khan-Huang-Liang (KHL) models, and observations are correlated with these models. Due to observed anisotropy in the plate material, specimens were machined with axes in the thickness (ND), rolling (RD), transverse to rolling (TD) and 45 degrees to rolling directions. Anisotropy in the material is fully characterized.

2. Predictions from two constitutive models (Johnson-Cook & Khan-Huang-Liang) are made and compared to the experimental results. Microstructure is measured using optical microscope and SEM.

This approach is schematically shown in Fig. 1. Table 1 gives the compositions of three alloys used in this study.

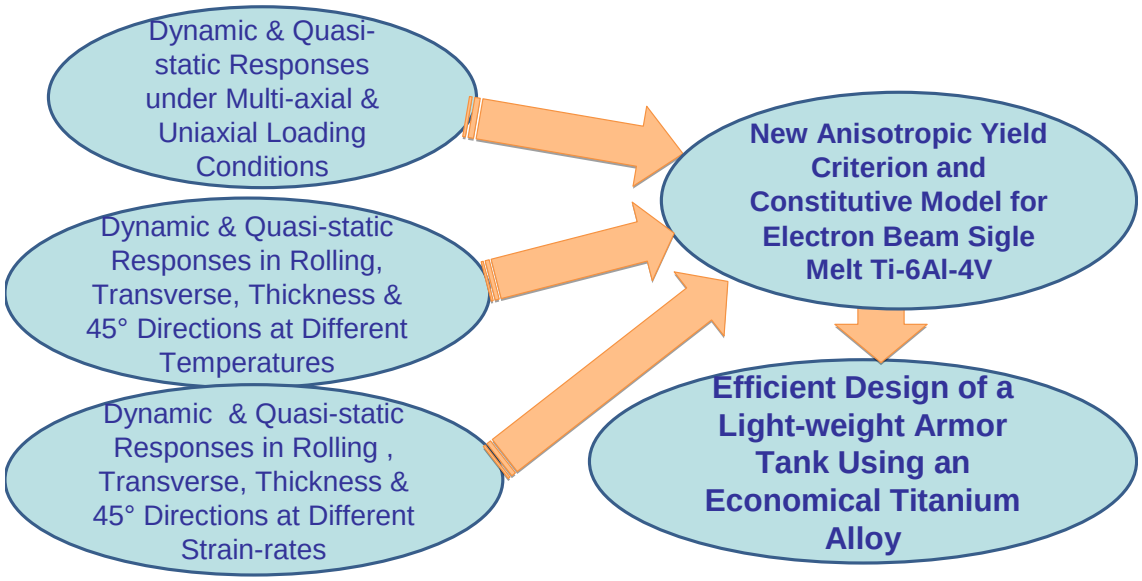

Fig. 1 The approach adopted for this project

Material	Al	V	Fe	Y	H	N	O	C	Ti	Oeq
Alloy 1	6.26	4.16	0.14	<0.0003	0.0031	0.008	0.178	0.047	REM	0.229
Alloy 2	6.30	3.86	0.18	<0.0003	0.0026	0.003	0.112	0.045	REM	0.152
Alloy 3	5.97	4.09	0.15	<0.0003	0.0041	0.008	0.174	0.043	REM	0.222

Table 1. Chemical composition of the three Ti-6Al-4V alloys used

BACKGROUND

This project will support the mission of TARDEC at Detroit and complement the basic research performed at the Army Research Lab. at Aberdeen on same or similar alloys.

Dynamic deformation has been of interest not only in impact and penetration related problems (Khan et al. 2004) but also in high speed machining (Molinari et al. 2002); titanium alloys have been studied by several investigators because of their use in aero-engine, gas turbines and other applications due to their high strength to weight ratio, ductility, and ability to withstand high temperatures and resist corrosion. The development of relatively economical Ti-6Al-4V alloy, with resulting high oxygen content, has sparked interest in its possible use in lightweight tanks (Montgomery and Wells, 2001); the conventional, more expensive Ti-6Al-4V alloy has been used primarily in aerospace components. The potential applications in armor, including ceramic tiles encapsulated in titanium alloys, have motivated several studies (Lesuer, 2000; Nemat-Nasser *et al*., 2001; Majorell *et al*., 2002).

In case of α-titanium, it has been demonstrated that the deformation mechanisms include glide systems with α-type dislocations in the HCP structure, as well as, twinning shear which contributed to the overall strain (Meyers *et al*., 1994; Song and Gray, 1995; Chichili *et al*., 1998). In the only quantitative study of twinning, Chichili *et al*. (1998) have shown that twin density increases drastically with increase in strain rate. The rate of increase of this density decreased with increase in strain at dynamic strain-rates of 10^3 s^{-1}, while this rate increased with deformation in the case of quasistatic loading (10^{-5} s^{-1}). Their results further demonstrated that loading at a particular temperature (and/or strain rate), unloading, and reloading at another temperature (and/or strain rate), resulted in a stress-strain curve which was significantly different than if the specimen was loaded at the latter temperature (and/or strain rate) right from the beginning. This study was performed over a wide range of strain rates (10^{-3}~10^3 s^{-1}) but over a very limited range of temperatures (77~298 K).

The Ti-6Al-4V alloy consists of HCP α-grains, with a dispersion of stabilized BCC β phase around grain boundaries at room temperature. α phase transforms to β phase starting at 873 K (1110 F); above 1268 K (1825 F), the entire microstructure consists of equiaxed β phase (Majorell *et al*., 2002). This alloy, in addition to H, V, and Ti, contains O, Fe, Mo, C, Si, and Mn. Oxygen, nitrogen, and carbon contents are α stabilizers (Conrad *et al*., 1975), while vanadium, iron and molybdenum are β stabilizers. Conrad *et al*. (1975) proposed an equivalent oxygen content (O_{eq} = O+2N+0.75C); this equivalent impurity concentration gives the effect of dislocations-impurity interaction on the yield strength of the material. Investigation by Majorell *et al*. (2002) was on an untextured and a textured Ti-6Al-4V alloy rod that was manufactured by Allvac. This study was over a

strain-rate range of 10^{-3} to 10 s^{-1} and a temperature range of 650~1345 K (710~1970 F). They did not observe any dynamic strain-aging at any of the temperatures or strain rates investigated. Further, athermal stress, *i.e.*, temperature insensitive response, was found at approximately 1255 K (1800 F); i.e. at a temperature when the material contained almost 100 % β phase. The equivalent oxygen content was 0.206 %.

In a study by Follansbee and Gray (1989), on a Ti-6Al-4V alloy, with an equivalent oxygen content of 0.23% (actual oxygen was 0.18%), the measurements were restricted to three temperatures with a range between 76 and 295 K and at only two strain rates (10^{-3} & approx. 3000 s^{-1}). Their specimens on as-received and two heat-treated versions were made from a 13.8 mm thick plate. This investigation did not include responses over a wide range of temperatures. Nemat-Nasser *et al*. (2001) study was on a commercial and two hot isostatically pressed Ti-6Al-4V alloys. The equivalent oxygen in the commercially pure alloy was 0.22 %. They performed experiments on specimens from 77 K to 998 K in the dynamic strain rate regime of 2000 to 4000 s^{-1}. As discussed earlier, α-phase starts transforming to β-phase at 873 K. Thus, they performed experiments on presumably different materials in their range of temperatures, *i.e.*, with different amounts of α and β phases. They suggested that all (*i.e.* 100 %) of plastic work done was converted to heat. This suggestion is in direct contradiction to the measurements of Mason *et al*. (1994), Macdougall and Harding (1999) and Rosakis *et al*. (2000).

The constitutive models used for high strain rate applications can be classified in two categories; the purely phenomenological ones, e.g. Johnson-Cook (J-C) (Johnson and Cook, 1983) and Khan-Huang-Liang (KHL) models (Khan and Huang, 1992; Khan and Liang, 1999; Khan et al., 2004) and so called, "physically based models" *e.g*. the ones by Zerilli and Armstrong (1987), Mecking and Kocks (1981), *etc.*, that were used frequently by Follansbee and Gray (1989), and in a modified form by Nemat-Nasser *et al.* (2001). The latter group discusses the mechanisms of plastic deformation (mainly dislocations). However, the material constants are determined by not measuring any deformation mechanism related quantity, but by choosing constants to "fit" the uniaxial stress-strain curves at different strain rates and temperatures, just like in the case of the purely phenomenological models. In the simplification or modification of this model by Nemat-Nasser *et al*. (2001), experiments are needed at very high temperatures where proper lubrication is extremely difficult, if not impossible to attain. Since in both categories of models, phenomenological and so called "physically based", material constants are determined by "fitting" to the stress-strain responses at different temperatures and strain rates, the advantage of one over the other is primarily the number of material constants in each model. Any model with a large number of material constants will be able to approximate observed responses. Mecking and Kocks model, as used by Follansbee and Gray (1989) has 23 constants, while these constants range from 12 to 8 in case of Cheng and Nemat-Nasser (2000) and Nemat-Nasser *et al.* (2001), respectively, depending on whether they include modeling of dynamic strain aging or not. Johnson-Cook and Khan-Huang-Liang models have 5 and 6 constants, respectively. Johnson-Cook and Khan-Huang-Liang models are used in this investigation due to their advantage of fewer constants and their ability to model the observed material response as closely as with models with many more constants. Also, Khan et al. (2004) have shown that the KHL

model has more flexibility than J-C model, and can accurately describe the observed responses in Ti-6Al-4V ELI and other titanium alloys.

SUMMARY OF IMPORTANT RESULTS

During projectile penetration in an armor material, it is subjected to deformations at high strain rates, temperatures and hydrostatic pressures. In this comprehensive study, the responses of the alloy were determined in three directions (to study anisotropy), at low to high temperatures (to determine temperature effect), at low to high strain rates (to quantify strain rate dependence), under tension and compression loading to investigate asymmetry in tension-compression, and compression response under changing hydrostatic pressure at different strain rates and different temperatures. Then some of the measured responses are modeled using KHL and JC constitutive equations.

Anisotropic Responses of the Material at Room Temp.

Fig. 2 shows the effect of anisotropy in the plane of the plate. The responses in compression were determined along rolling and transverse to rolling directions (RD & TD), as well as at different angular directions from RD at a strain rate of 10^{-4} per second. The rolling direction shows higher yield stress than transverse direction with other angular direction responses falling in-between RD & TD. The work hardening rate appears to be almost same in all directions.

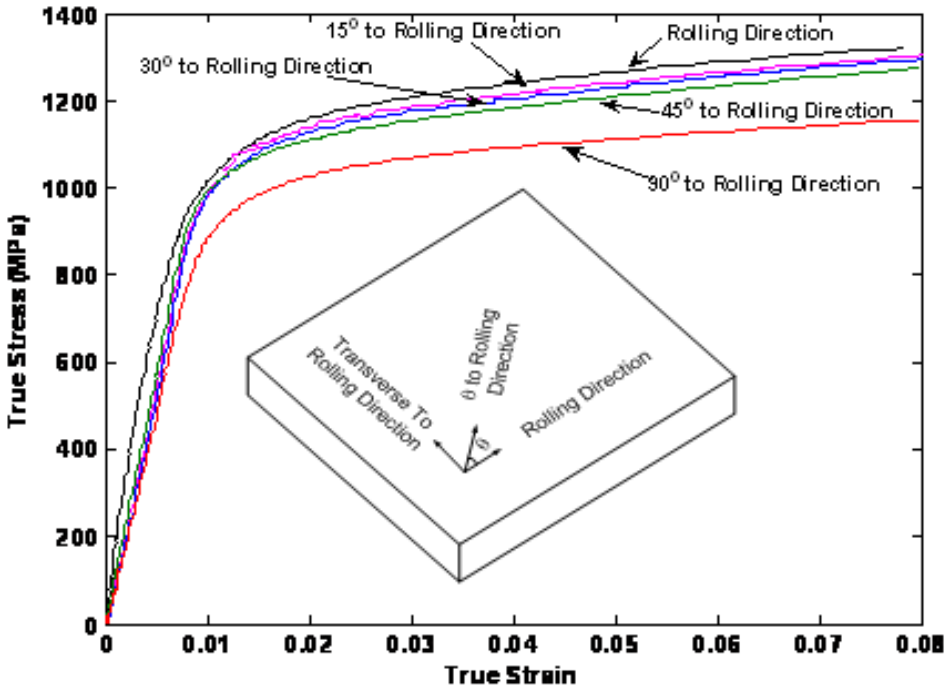

Fig. 2 Responses of the alloy in different directions of the plate, rolling direction (RD), transverse to the rolling direction (TD, 90^0 to the rolling direction) and three directions in between these two directions.

In Fig. 3 the anisotropy of the material is shown at two high (dynamic) and three low (quasi-static) strain rates in RD, TD and ND (normal to RD & TD, normal to plate surface) directions. The strain rates were of the order of 10^{3}, 10^{-4}, 10^{-2}, 10^{0} per second. The response in the rolling direction is much higher than the ones in transverse and thickness directions; the responses are almost same in the two latter directions. Further, a strong strain rate effect is visible in this Fig. In order to follow responses in a particular direction, a different color is used for each direction. The strain rate effect varies nonlinearly with increase in the strain rate.

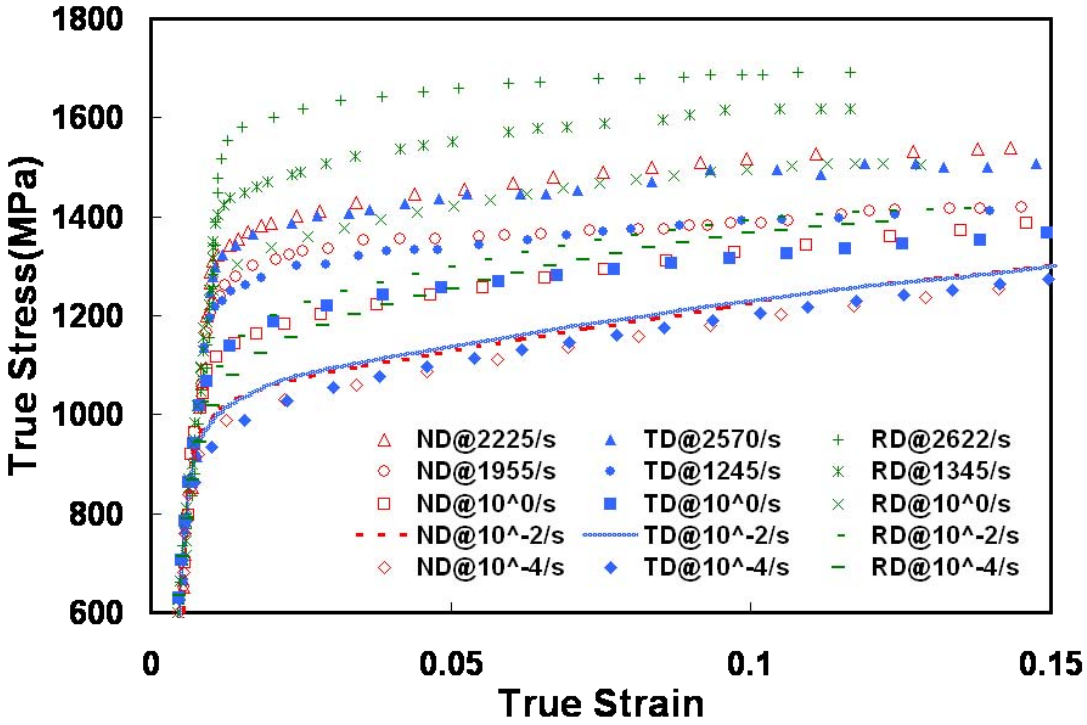

Fig.3 Anisotropic responses under compression in three directions at 296K, and at different strain rates in quasi-static and dynamic regimes.

Temperature Dependent Anisotropic Responses

Next Fig. contains responses along the rolling (RD), transverse (TD) and thickness, or normal (ND) directions at different temperatures at a strain rate of 10^{-3} per second. The temperatures were 233, 296, 422, 589 & 755 K. Again, the response in each direction is shown by a different color. The anisotropy is observed to depend non-linearly on the temperature; this dependence is stronger than the strain rate effect in the earlier Fig .

The measured anisotropic responses at high strain rates are shown in Figs. 5 & 6. The strain rates of responses shown in these Figs. increase from approximately 1000 to around 3000 per sec. These dynamic responses were measured using compression Split Hopkinson Bar (SHB) technique at low and high temperatures. These responses are visibly very non-linearly dependent on strain rates and temperatures.

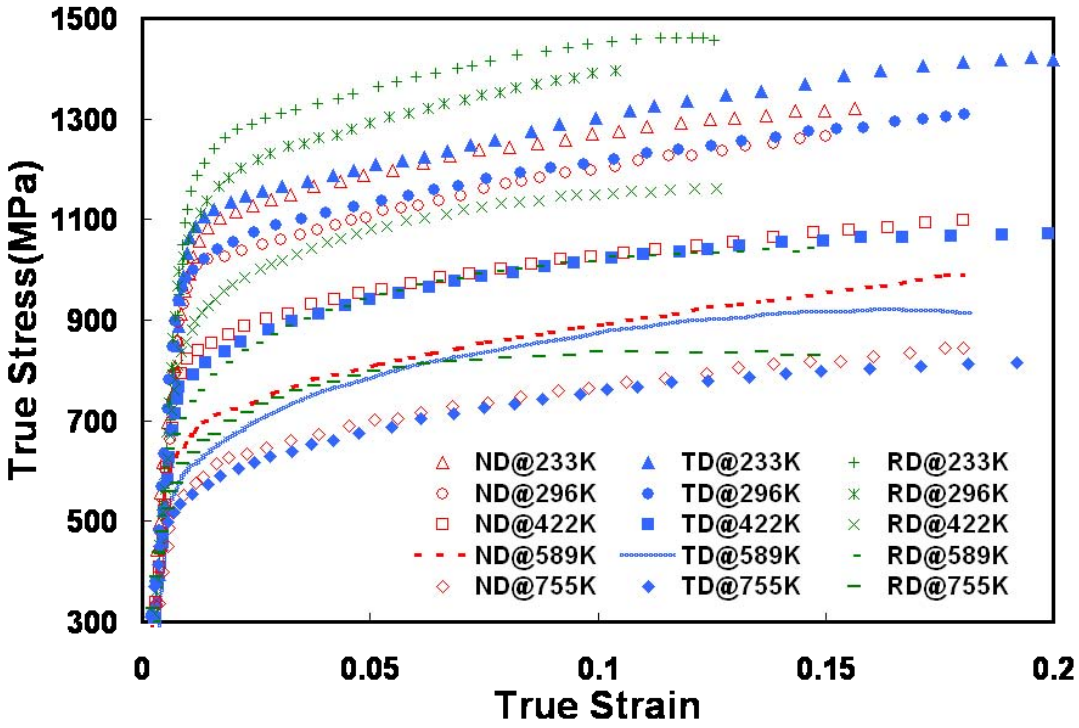

Fig. 4 Temperature dependent anisotropic responses under compression in three directions, at a constant strain rate of 10^{-3} s^{-1}.

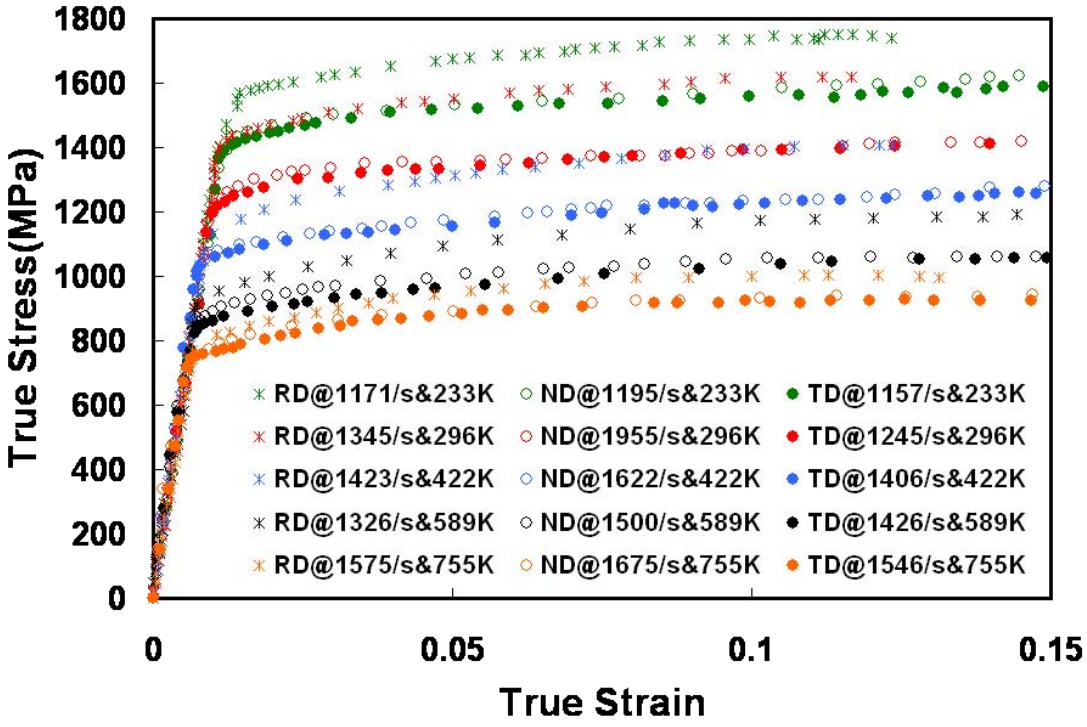

Fig. 5 Different anisotropic responses in dynamic compression (at strain rates from 1157 to 1955 s^{-1}), in three directions; measured results at 233, 296, 422, 598 & 755K are shown using green, red, blue, black and orange symbols, respectively.

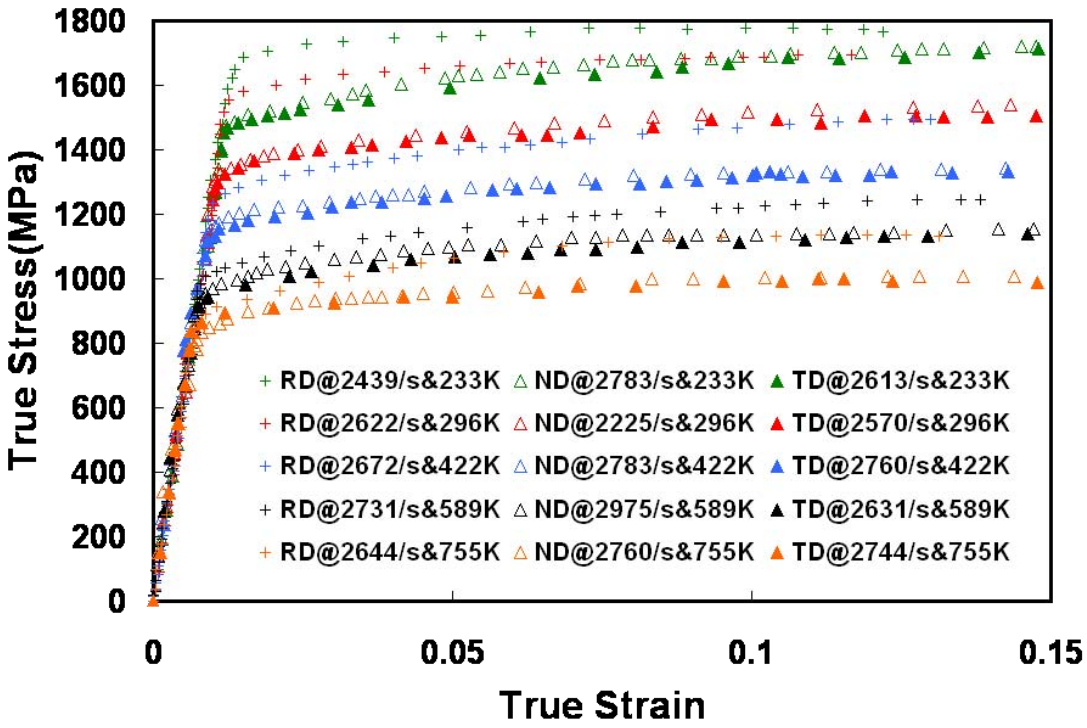

Fig. 6 Different anisotropic responses in dynamic compression (at strain rates from 2225 to 2975 s^{-1}), in three directions; measured results at 233, 296, 422, 598 & 755K are shown using green, red, blue, black and orange symbols, respectively.

Tension-Compression Asymmetry

The behavior of the alloy is significantly different in tension and compression as shown in Fig. 7 from experiments with loading in the rolling direction. There is an appreciable difference not only in yield stress levels but also in work hardening. These differences are further exemplified in next Fig. where anisotropic responses in tension and compression are shown at the room temperature at strain rates in quasi-static loading regime. The failure strains in tension are slightly lower than in compression; the failure strains in thickness (ND) direction in compression loading are much higher than rolling direction (RD), while failure strains in the transverse to rolling direction (TD) are in between the other two directions.

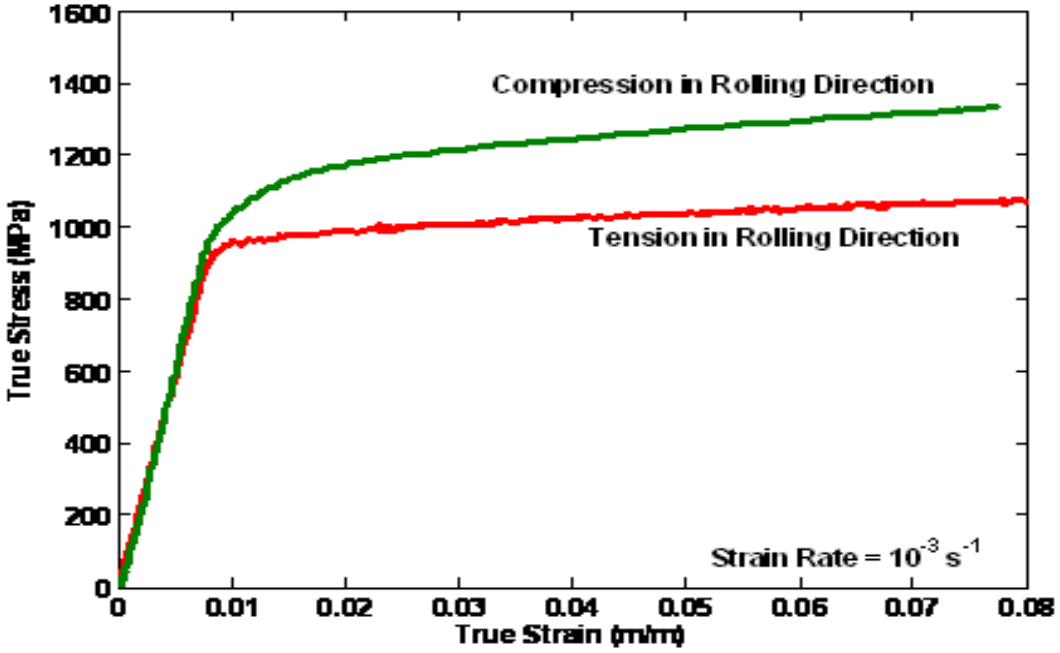

Fig. 7 Different responses in tension and compression loading along the rolling direction.

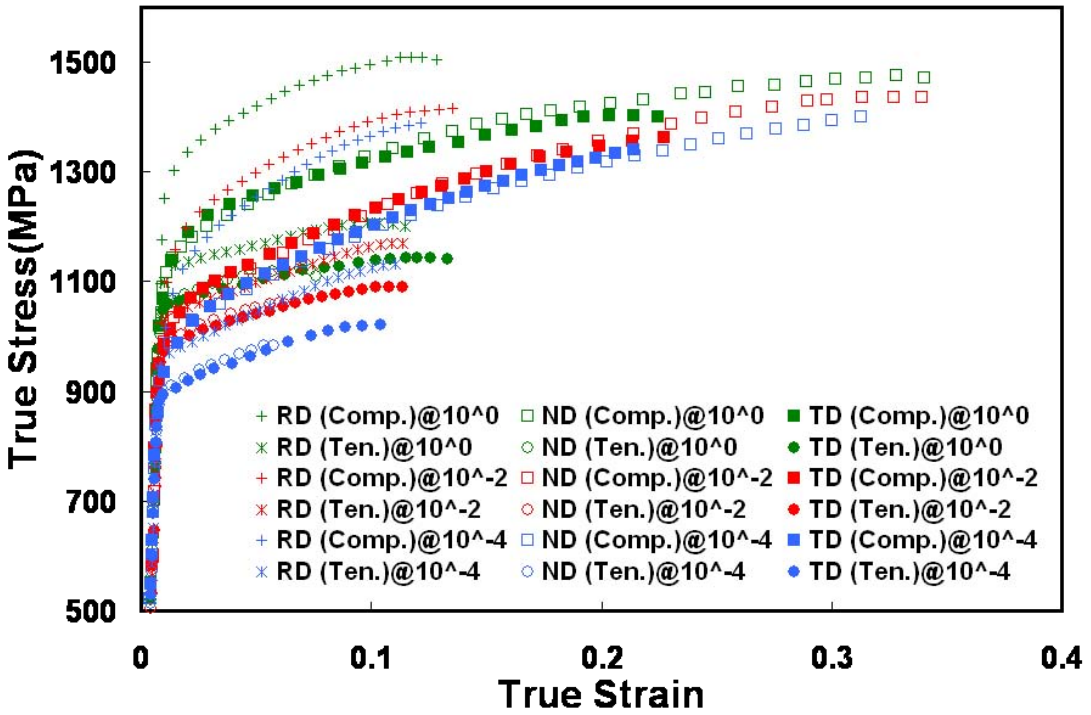

Fig. 8 Different anisotropic responses in tension and compression, in three directions at 296K; experimental results at a strain rate of 10^{0}, 10^{-2} and 10^{-4} s^{-1}, are shown in green, red and blue colors, respectively.

Material Responses Under Confining Pressure

In Fig. 9, the responses of the alloy under confining pressure are shown at different confining pressures and four different strain rates in the rolling direction. These experiments were performed with the specimens loaded in compression inside a pressure vessel, thus the cylindrical surface of the specimens were subjected to a hydrostatic or confining pressure. The pressure inside the pressure chamber was changed to get different confining pressures. The stress-strain curves appear to shift by the amount of confining pressure. These measured responses are re-plotted in terms of von Mises equivalent stress and strain in next Fig., there is almost negligible effect of the hydrostatic pressure at these low hydrostatic pressures; however the failure strains increase with increase in hydrostatic pressure (not shown in these Figs.). Similar measured responses in TD and ND directions are shown in Figs. 11 and 13, respectively in terms of stress and strain; Figs. 12 and 13 contain the same measured responses in terms of von Mises equivalent stress and strain.

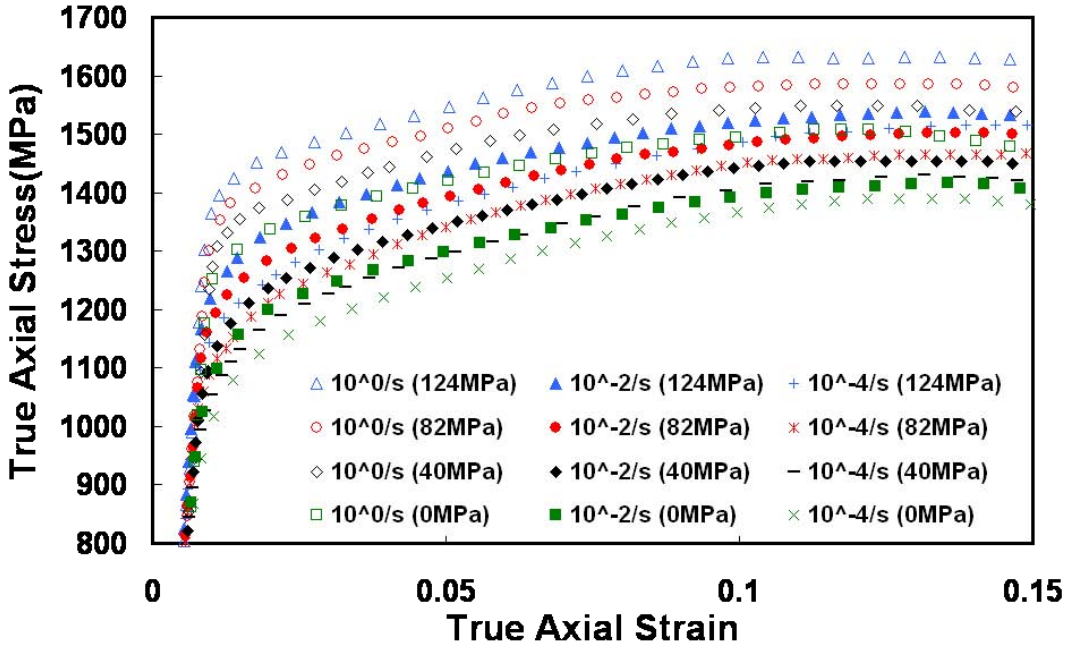

Fig. 9 Measured responses in compression along rolling direction (RD), under different confining pressures ranging from 0 to 124 MPa.

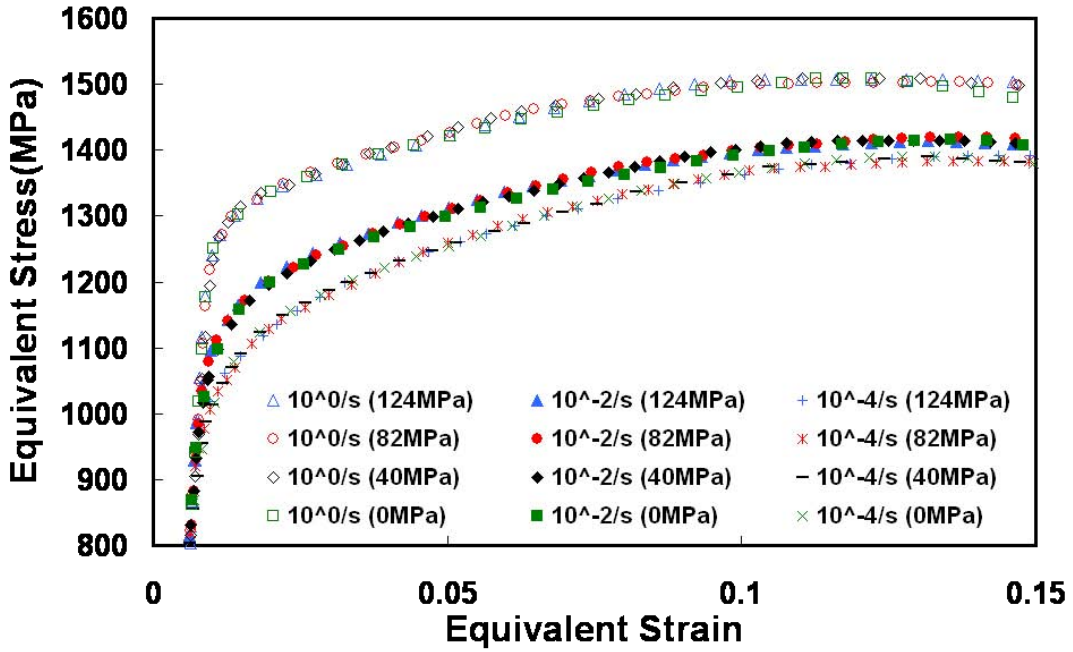

Fig. 10 Responses in compression along rolling direction (RD), under different confining pressures ranging from 0 to 124 MPa, in terms of equivalent stresses and strains.

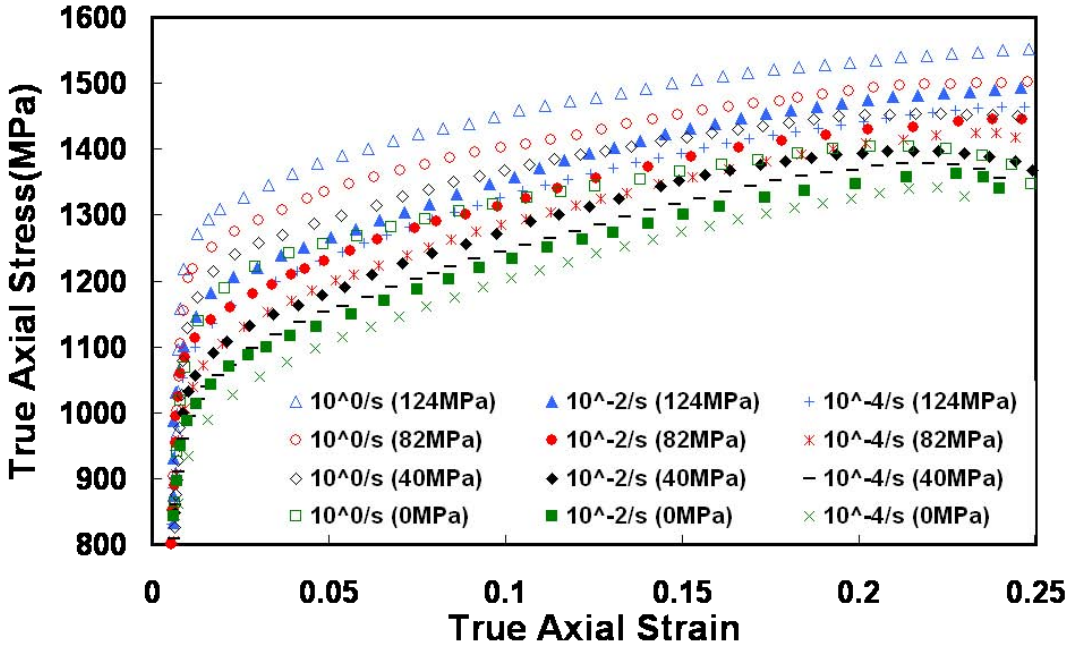

Fig. 11 Measured responses in compression along transverse to rolling direction (TD), under different confining pressures ranging from 0 to 124 MPa.

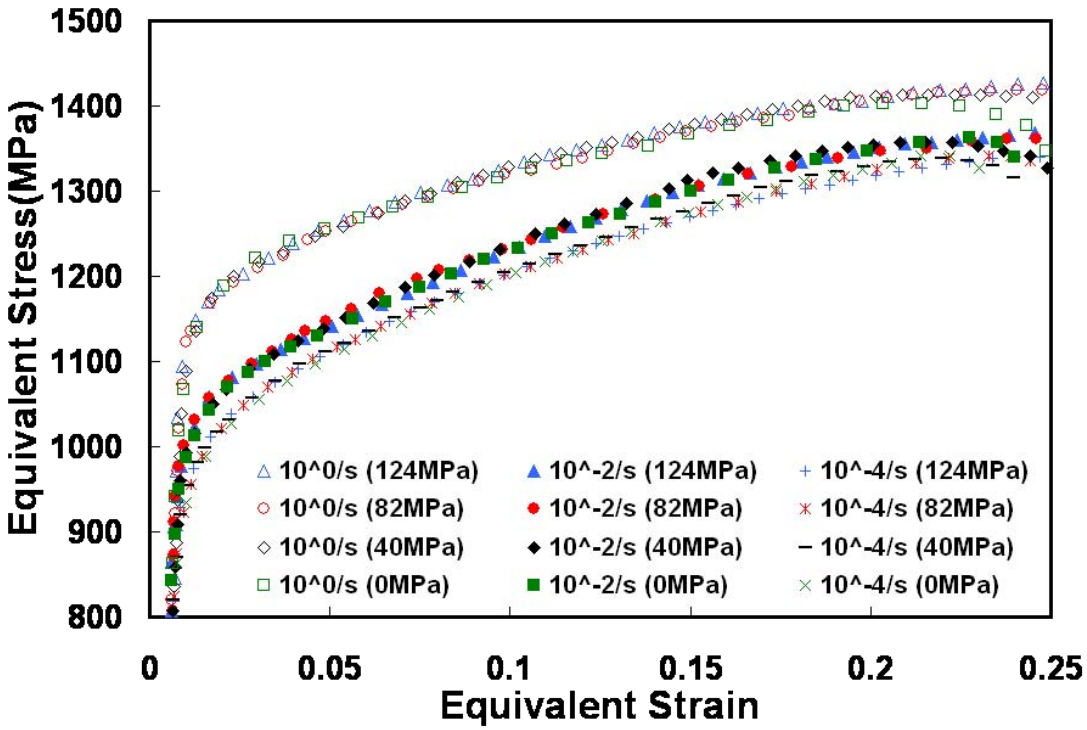

Fig. 12 Responses in compression along transverse to rolling direction (TD), under different confining pressures from 0 to 124 MPa, in terms of eq. stresses and strains.

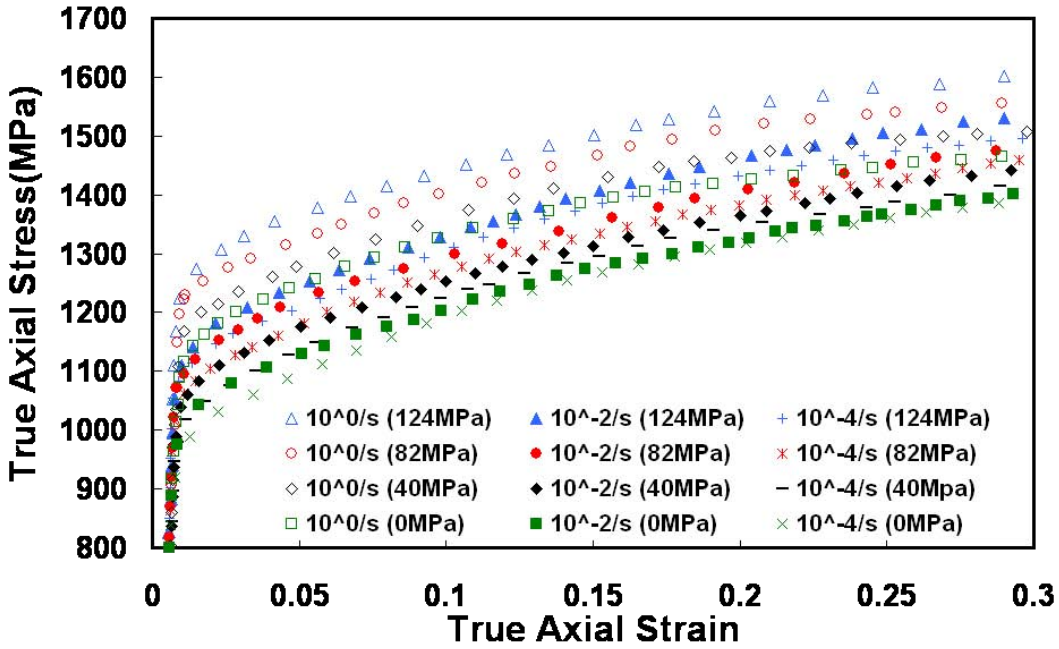

Fig. 13 Measured responses in compression along normal to rolling plane (ND), or through thickness direction, under different confining pressures from 0 to 124 MPa.

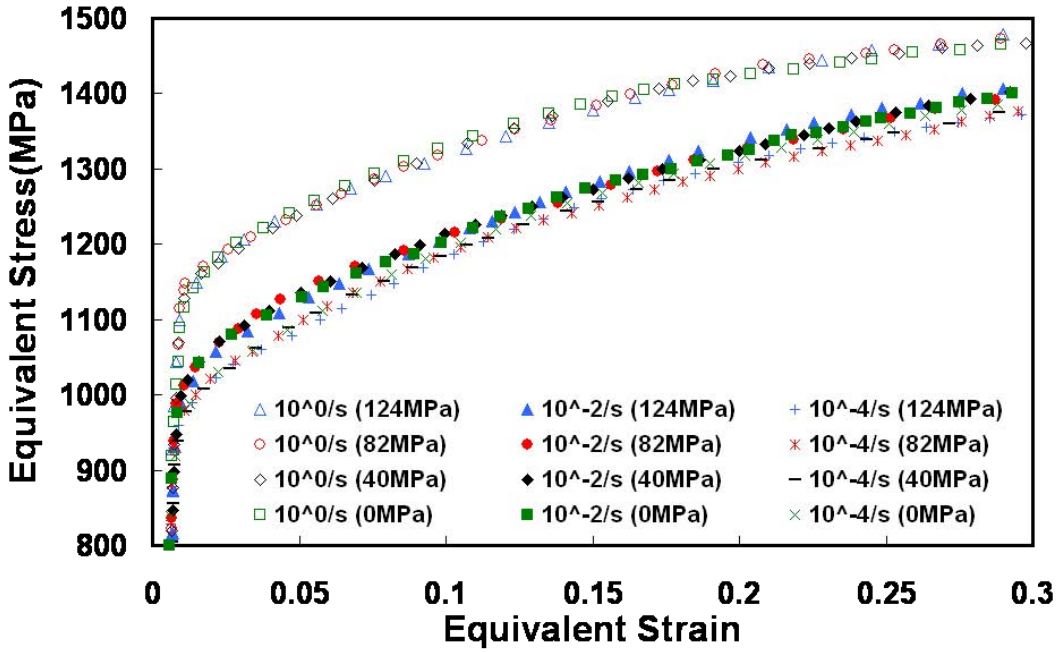

Fig. 14 Responses in compression along normal to rolling plane (ND), or through thickness direction, under different confining pressures ranging from 0 to 124 MPa, in terms of equivalent stresses and strains.

Constitutive Modeling

The material constants for both, the modified KHL and JC models were determined. Using these material constants, correlations were obtained and compared to experimental results. The modified KHL model is as follows:

$$\sigma = \left[A + B\left(1 - \frac{ln\,\dot{\varepsilon}}{ln\,D_0^p} \right)^{n_1} \varepsilon_p^{\,n_0} \right] \left(\frac{\varepsilon}{\dot{\varepsilon}^*} \right)^c \left(\frac{T_m - T}{T_m - T_{ref}} \right)^m \tag{1}$$

where, σ is the true (Cauchy) stress and ε^p is the true plastic strain. T_m, T, T_{ref} are melting, current, and reference temperatures, respectively. $D_0^p = 10^6$ s^{-1} (arbitrarily chosen upper bound strain rate) and $\dot{\varepsilon}^* = 1$ s^{-1}(reference strain rate, at a reference temperature of T_{ref}, usually room temperature, at which material constants A, B and n_0 are determined). $\dot{\varepsilon}$ is the current strain rate. n_1, C and m are additional material constants. For Ti-6Al-4V alloys, the melting temperature was taken to be 1933 K (ASM handbook, 1994). The reference temperature was the constant room temperature for experiments at 296K.
The JC model which has been used previously is given as follows:

$$\sigma = \left[A + B\left(\varepsilon^p \right)^{n_0} \right] \left(1 + C \ln \frac{\dot{\varepsilon}}{\dot{\varepsilon}^*} \right) \left(1 - \left(\frac{T - T_r}{T_m - T_r} \right)^m \right) \tag{2}$$

The KHL model has two distinct advantages over the JC model. These are the addition of another material constant, n_1, which is able to simulate the decreasing work hardening behavior of certain materials with increase in strain rate. The second advantage is the modified temperature term which enables to simulate the material behavior below the reference temperature T_{ref}. In the JC model the temperature term cannot accommodate the case when the current temperature is lower than the reference temperature as then the above term within parenthesis becomes a negative number raised to the power *m*. The model material constants are determined through systematic procedure and further refined using least square optimization technique. An illustrative example of the modeling using JC and KHL is shown in Fig. 15 for one of the alloys studied during the current investigation. The figure clearly shows the capability of the KHL model against the JC model in predicting the material behavior under different loading conditions. The material constants determined from uniaxial experiments are given in Table 2.

	A **(MPa)**	***B*** **(MPa)**	n_1	n_0	***C***	***M***
Ti-6Al-4V Alloy 1	1100	857.5	0.5455	0.6086	0.02204	1.6236
Ti-6Al-4V Alloy 2	988	747.1	0.5455	0.3986	0.02204	1.2214
Ti-6Al-4V Alloy 3	1069	874.8	0.5455	0.4987	0.02204	1.3916

Table 2. KHL model material constants determined for the three Ti-6Al-4V Alloys used in the investigation

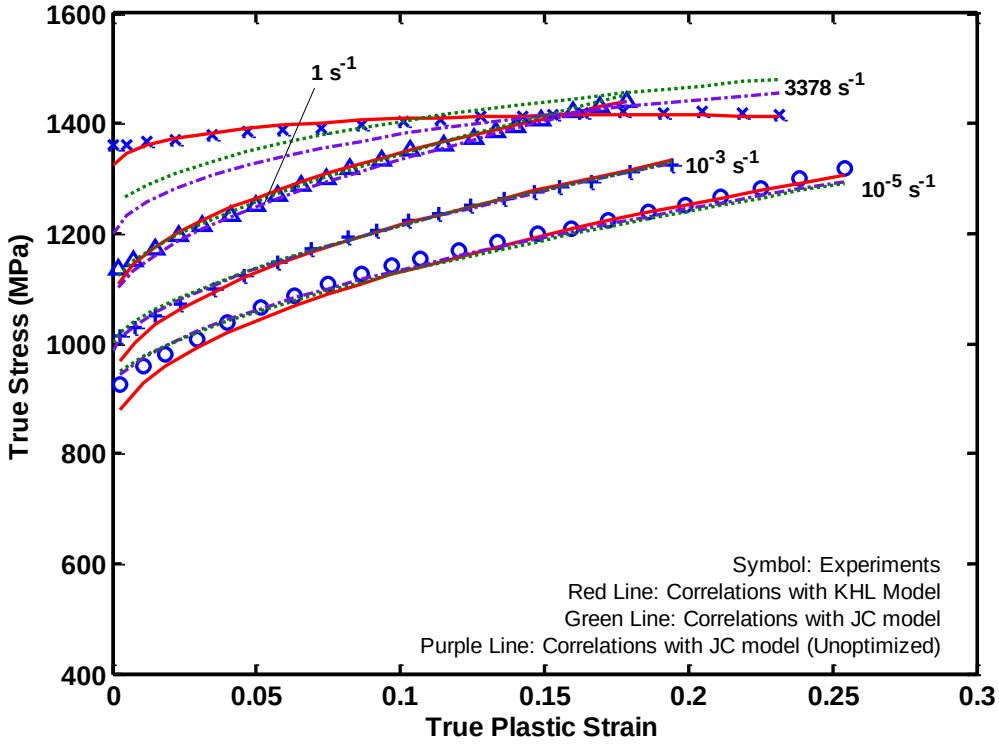

Fig. 15 Comparisons between KHL model and JC model correlations for alloy 3 studied in the investigation at room temperature and different strain rates.

To determine the temperature dependence in the KHL and JC models, experiments were performed on a titanium alloy at different temperatures. The temperatures chosen for these experiments were both above and below the reference temperature which in this case was room temperature, but below $0.4T_m$. The experimental observations along with the model correlations are shown in Fig 16. Note the absence of any JC correlation for the experiment performed below the reference temperature of 233K; the KHL model is able to correlate the material response for that experiment also quite well. Overall, the KHL model was able to simulate the material behavior at these temperatures reasonably well whereas JC was unable to simulate for certain temperatures; also the correlations obtained through JC model were also not as good as the ones obtained by using KHL.

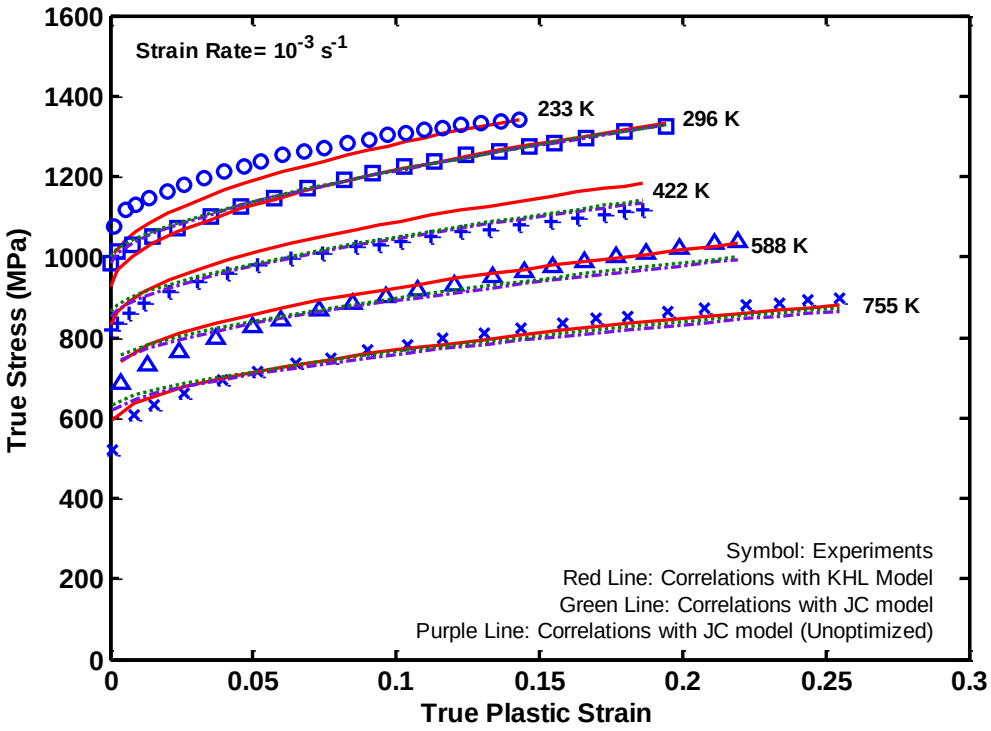

Fig. 16 KHL and JC model correlations for experiments performed at different temperatures for alloy 3 at the strain rate of 10-3 s-1. Note the absence of correlation at 233Kwith JC model in which the temperature term $(T\text{-}T_{ref})/(T_m\text{-}T_{ref})$ becomes negative.

From this investigation it is found that Ti–6Al–4V is non-linearly dependent on strain rate, as well as temperature. The KHL model is found to correlate better than JC model especially during dynamic deformation regime. The thermal softening at high strain rates, together with reduction in the work hardening rate with increase in strain rate and strain, is captured much better by the KHL model than the JC model. The temperature term of the modified KHL viscoplastic constitutive model is able to correlate well with the response at a temperature (233 K) which is lower than the reference temperature (296 K); the JC model is not valid in this case.

Bibliography

Cheng, J., Nemat-Nasser, S., 2000. A model for experimentally-observed high-strain-rate dynamic strain aging in titanium. Acta Materialla 48 (12), 3131-3144.

Chichili, D. R., Ramesh, K. T., Hemker, K. J., 1998. The high strain rate response of

Alpha-Titanium: Experiments, deformation mechanisms and modeling. Acta Meterialia 46 (3), 1025-1043.

Conrad, H., M., Doner, M., de Meester, B., 1973. Critical review deformation and fracture. In: International Conference on Titanium, Proceedings of Titanium Science and Technology, Massachusetts Institute of Technology, Boston, p. 969.

Harding, J., " The temperature and strain rate sensitivity of a-titanium", *Archive of Mechanics*, 27, p. 715, 1975.

Johnson, G. R., Cook, W. H., 1983. A constitutive model and data for metals subjected to large strains, high strain rates and high temperatures. In: Proceedings of the Seventh International Symposium on Ballistic, The Hague, The Netherlands, 1983, p. 541.

Khan, A. S., Liang, R., 1999. Behaviors of three BCC metal over a wide range of strain rates and temperatures: Experiments and modeling. International Journal of Plasticity, 15 (9), 1089-1109.

Khan, A. S., Suh, Y. and Kazmi, R., 2004. Quasi-static & Dynamic Loading Responses and Constitutive Modeling of Titanium Alloys, International Journal of Plasticity, 20, 2233-2248.

Khan, A. S., Kazmi, R. & Farrokh, B., Multiaxial & Non-proportional Loading Response, Anisotropy and Modeling of Ti-6al-4v titanium Alloy Over Wide Ranges of Strain Rates and Temperatures, International Journal of Plasticity, Vol. 23, pp. 931-950, *2007*.

Khan, A. S., Kazmi, R. & Farrokh, B., and Zupan, M., Effect of Oxygen Content and Microstructure on the Thermo-mechanical Response of Three Ti-6Al-4V alloys: Experiments and Modeling Over a Wide Range of Strain-rates and Temperatures, International Journal of Plasticity, Vol. 23, pp. 1105-1125, *2007*.

Lesuer, D. R.. 2000. Experimental investigations of material models for Ti-6Al-4V Titanium and 2024-T3 Aluminum. In: Final Report, DOT/FAA/AR-00/25, U. S. Department of Transportation, Federal Aviation Administration.

Macdougall, D. A. S., Harding, J., 1999. A constitutive relation and failure criterion for Ti6Al4V alloy at impact rates of strain. Journal of the Mechanics and Physics of Solids 47 (5), 1157-1185.

Majorell, A., Srivatsa, S., Picu, R. C., 2002. Mechanical behavior of Ti-6Al-4V at high and moderate temperatures - Part I: Experimental results. Materials Science and Engineering A326 (2), 297-305.

Mason, J. J., Rosakis, A. J., Ravichandran, G., 1994. On the strain and strain rate dependence of the fraction of plastic work converted into heat: An experimental study

using high speed infrared detectors and the Kolsky bar. Mechanics of Materials 17 (2-3), 135-145.

Meyers, M. A., Subhash. G., Kad, B. K., Prasad, L. 1994. Evolution of microstructure and shear-band formation in A-hcp titanium. Mechanics of Materials 17 (2-3), 175-193.

Molinari, A., Musquar, C. and Sutter, G., 2002. Adiabatic shear banding in high speed machining of Ti-6Al-4V: experiments and modeling, International Journal of Plasticity, 18(4), 443-459.

Montgomery, J. S., Wells, M. G. H., 2001. Titanium armor applications in combat vehicles. JOM, 53 (4), 29-32.

Nemat-Nasser, S., Guo, Wei-Guo, Nesterenko, Vitali F., Indrakanti, S. S., Gu, Ya-Bei, 2001. Dynamic response of conventional and hot isostatically pressed Ti-6Al-4V alloys: Experiments and modeling. Mechanics of Materials, 33 (8), 425-439.

Rosakis, P., Rosakis, A. J., Ravichandran, G., Hodowany, J., 2000. A thermodynamic internal variable model for the partition of plastic work into heat and stored energy in metals. Journal of Mechanics and Physics of Solids 48 (3), 581-607.

Song, S. G., Gray III, G. T., 1995. Structural interpretation of the nucleation and growth of deformation twins in Zr and Ti - I. Application of the coincidence site lattice (CSL) theory to twinning problems in H.C.P. structures. Acta metall. mater. 43 (6), 2325-2337.

Zerilli, F. J., Armstrong, R. W., 1987. Dislocation-mechanics-based constitutive relations for material dynamics calculations. Journal of Applied Physics 61 (5), 1816-1825.